https://doi.org/10.1038/s41586-019-1274-4

De novo protein design by citizen scientists

Brian Koepnick[1,2], Jeff Flatten[3], Tamir Husain[3], Alex Ford[1,2], Daniel-Adriano Silva[1,2], Matthew J. Bick[1,2], Aaron Bauer[3], Gaohua Liu[4,5], Yojiro Ishida[6], Alexander Boykov[11], Roger D. Estep[11], Susan Kleinfelter[11], Toke Nørgård-Solano[11], Linda Wei[11], Foldit Players[10], Gaetano T. Montelione[4,6], Frank DiMaio[1,2], Zoran Popović[3], Firas Khatib[7], Seth Cooper[8] & David Baker[1,2,9]*

Online citizen science projects such as GalaxyZoo[1], Eyewire[2] and Phylo[3] have proven very successful for data collection, annotation and processing, but for the most part have harnessed human pattern-recognition skills rather than human creativity. An exception is the game EteRNA[4], in which game players learn to build new RNA structures by exploring the discrete two-dimensional space of Watson–Crick base pairing possibilities. Building new proteins, however, is a more challenging task to present in a game, as both the representation and evaluation of a protein structure are intrinsically three-dimensional. We posed the challenge of de novo protein design in the online protein-folding game Foldit[5]. Players were presented with a fully extended peptide chain and challenged to craft a folded protein structure and an amino acid sequence encoding that structure. After many iterations of player design, analysis of the top-scoring solutions and subsequent game improvement, Foldit players can now—starting from an extended polypeptide chain—generate a diversity of protein structures and sequences that encode them in silico. One hundred forty-six Foldit player designs with sequences unrelated to naturally occurring proteins were encoded in synthetic genes; 56 were found to be expressed and soluble in *Escherichia coli*, and to adopt stable monomeric folded structures in solution. The diversity of these structures is unprecedented in de novo protein design, representing 20 different folds—including a new fold not observed in natural proteins. High-resolution structures were determined for four of the designs, and are nearly identical to the player models. This work makes explicit the considerable implicit knowledge that contributes to success in de novo protein design, and shows that citizen scientists can discover creative new solutions to outstanding scientific challenges such as the protein design problem.

The principle underlying de novo protein design is that proteins fold to their lowest free-energy state[6]; hence, designing a new protein structure requires finding an amino acid sequence with its lowest energy state in the prescribed structure. In practice, this challenge can be divided into two subproblems: first, crafting a protein backbone that is designable (that is, that could be the lowest energy state of some sequence); and second, finding a sequence with its lowest energy state in the crafted structure. One of the challenges of protein design is the exponentially increasing number of conformations available to a polypeptide chain, which is huge even for a modestly sized protein of 60–100 residues. Thus, the first subproblem of crafting a plausible backbone is extremely open-ended, and the second subproblem is difficult because it is not tractable to explicitly check that a designed sequence has lower energy in the crafted structure than in any other structure. There has been considerable progress in de novo protein design in recent years[7–10], but it is unclear whether all of the contributions to this success have been made explicit in the protocols used to design proteins, and how much implicit knowledge resides in the expertise of the designers. Disentangling the role of expert knowledge is particularly difficult for the extremely open-ended challenge posed by the first subproblem (that is, crafting a plausible backbone), for which there are a practically unlimited number of solutions. Because full computer enumeration of backbones is not possible, there is considerable room for human creativity and intuition in generating and designing new protein structures.

To investigate how crowd-based creativity could contribute to solving the de novo protein design problem, we incorporated de novo design tools into the protein-folding game Foldit. Foldit is a free online computer game developed to crowdsource problems in protein modelling, and provides full control over the three-dimensional structure of a protein model[5] (Fig. 1). Players compete to build a model with the lowest free energy, as calculated using the Rosetta energy function[11]. In the past, Foldit has been primarily applied to protein structure prediction problems, in which players are presented with an unstructured amino acid sequence and challenged to determine its native conformation[5,12]. In one case, Foldit players redesigned a loop region of an already folded structure[13], but the de novo design of an entire protein is a far more expansive challenge.

We repeatedly challenged Foldit players to design stably folded proteins from scratch, and iteratively improved the game on the basis of their results. In each challenge, players were provided with a polyisoleucine backbone in a fully extended conformation (60–100 residues in length) and were given 7 days to fold the backbone into a compact structure and identify a sequence specifying this backbone. Initially, most top-scoring (low-energy) Foldit player designs were highly extended, lacked a solvent-inaccessible core and were composed entirely of polar residues (Extended Data Fig. 1); such extended, fully α-helical structures have more favourable hydrogen bonding, electrostatic and local torsional energies than collapsed structures, which must contort to create a buried core. Whereas polylysine and other extended polar sequences resembling these initial Foldit solutions are often α-helical in solution[14,15], the lack of long-range interactions precludes specific folding into a single stable structure[16]. This highlights a limitation of using absolute energy as an optimization criterion for protein design: a low-energy design does not guarantee structural specificity, which arises only if all other alternative conformations have higher energy. To favour the design of globular solvent-excluding protein folds, with sequences that uniquely encode them, we introduced three supplementary design rules into Foldit: a ‘core exists’ rule that requires a minimum proportion of residues (for example, 30%) to be solvent-inaccessible in the designed structure; a ‘secondary structure design’ rule that prohibits glycine and alanine in all secondary structure elements; and a ‘residue interaction energy’ rule to penalize large residues that make insufficient intramolecular interactions in the designed structure. With the addition of these rules to Foldit, subsequent top-scoring designs from Foldit players were compact globular proteins.

[1]Department of Biochemistry, University of Washington, Seattle, WA, USA. [2]Institute for Protein Design, University of Washington, Seattle, WA, USA. [3]Center for Game Science, Paul G. Allen School of Computer Science and Engineering, University of Washington, Seattle, WA, USA. [4]Department of Molecular Biology and Biochemistry, Rutgers University The State University of New Jersey, Piscataway, NJ, USA. [5]Nexomics Biosciences, Bordentown, NJ, USA. [6]Department of Biochemistry, Robert Wood Johnson Medical School, Rutgers The State University of New Jersey, Piscataway, NJ, USA. [7]Department of Computer and Information Science, University of Massachusetts Dartmouth, Dartmouth, MA, USA. [8]Khoury College of Computer Sciences, Northeastern University, Boston, MA, USA. [9]Howard Hughes Medical Institute, University of Washington, Seattle, WA, USA. [10]A list of participants appears in the Supplementary Information. [11]Unaffiliated: Alexander Boykov, Roger D. Estep, Susan Kleinfelter, Toke Nørgård-Solano, Linda Wei. *e-mail: dabaker@uw.edu

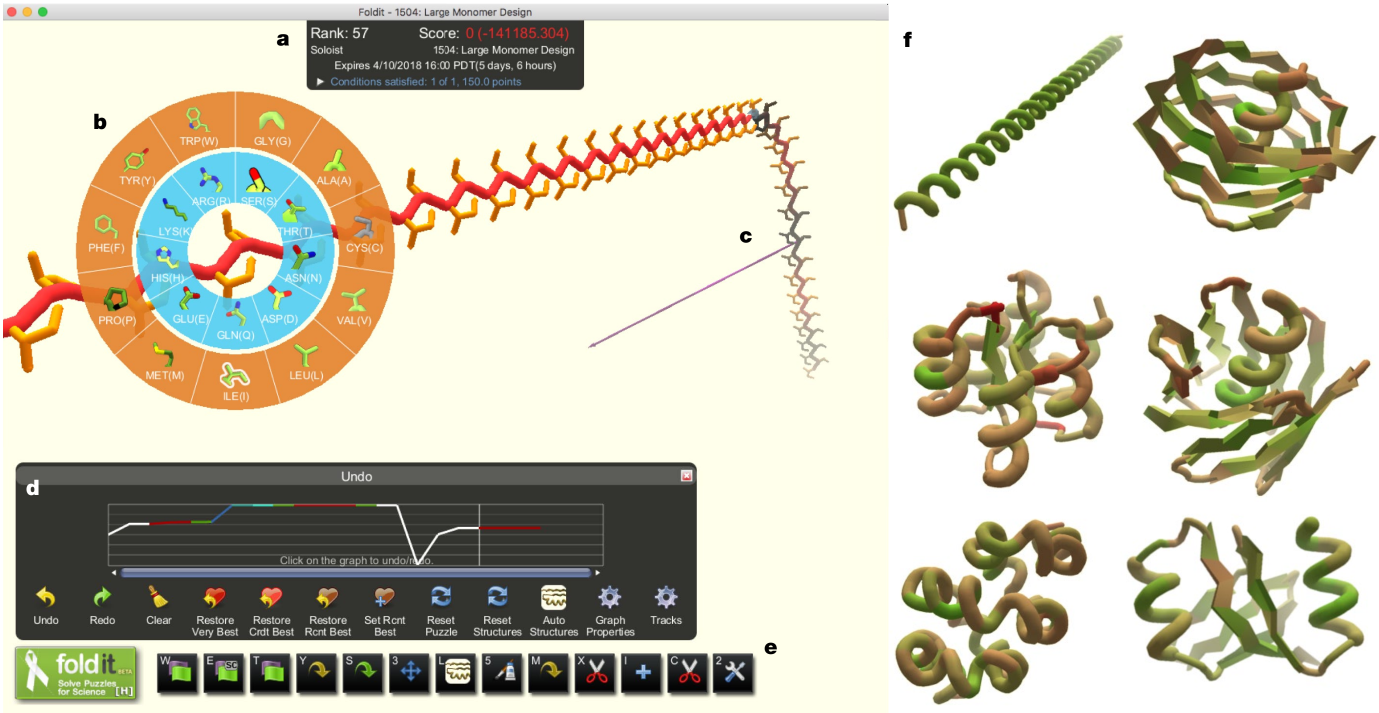

Fig. 1 | The Foldit user interface. a, The Foldit score is the Rosetta energy with a negative multiplier, so that better models yield higher scores. **b**, The design palette allows players to change the identity of the amino-acid residue at any position of the model. **c**, The ‘pull’ tool allows players to manipulate the 3D structure of the model. **d**, The ‘undo’ graph tracks the score as a model is developed, and allows players to backtrack and load previous versions of a model. **e**, Additional Foldit tools (from left to right): full-structure minimization, sidechain minimization, backbone minimization, auto-design sidechains, repack sidechains, translate or rotate model, secondary structure assignment, idealize secondary structure, manually design sidechains, delete residues, insert residues, insert cutpoint and idealize peptide bond geometry. **f**, Foldit players explore diverse structures that have no sequence or structural homology to natural proteins.

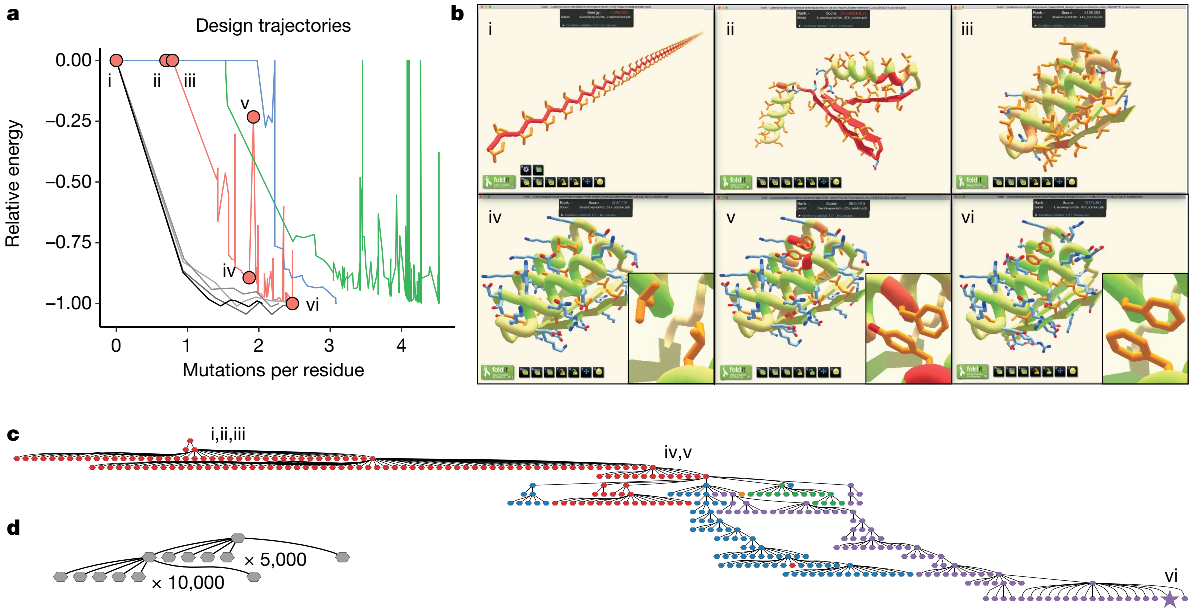

Fig. 2 | Comparison of Foldit player and automated design-sampling strategies. a, Single trajectories (ignoring abandoned branches) for three Foldit player-designed proteins in red (Foldit1), blue (Peak6) and green (Ferredog-Diesel); and design trajectories for four Rosetta-designed proteins in grey. The *y* axis is the Rosetta energy rescaled so that the final design has a value of −1.00, and positive energies are shown as zero. Foldit players are willing to undergo large increases in energy to explore new regions; by contrast, the Rosetta protocol has a limited ability to escape local energy minima. Red circles correspond to structures shown in **b**. **b**, Snapshots from the design trajectory of Foldit1: (i) the initial extended chain of polyisoleucine; (ii) development of secondary structure; (iii) development of folded tertiary structure; (iv) sequence design of folded structure, with inset showing favourable packing at positions 13 and 45; (v) high-energy intermediate design, with inset showing redesign at positions 13 and 45, which results in steric clashes with the protein backbone; (vi) the final refined design, with inset showing renewed favourable interactions at positions 13 and 45. **c**, The design strategy for Foldit1 represented as a graph, showing all branch points where multiple design trajectories were spawned from a single intermediate. The final design was reached after 17 branch points. Node colours correspond to five different cooperating Foldit players, and the final design is marked with a star. **d**, Similar representation of a Rosetta design trajectory—there are only two branch points.

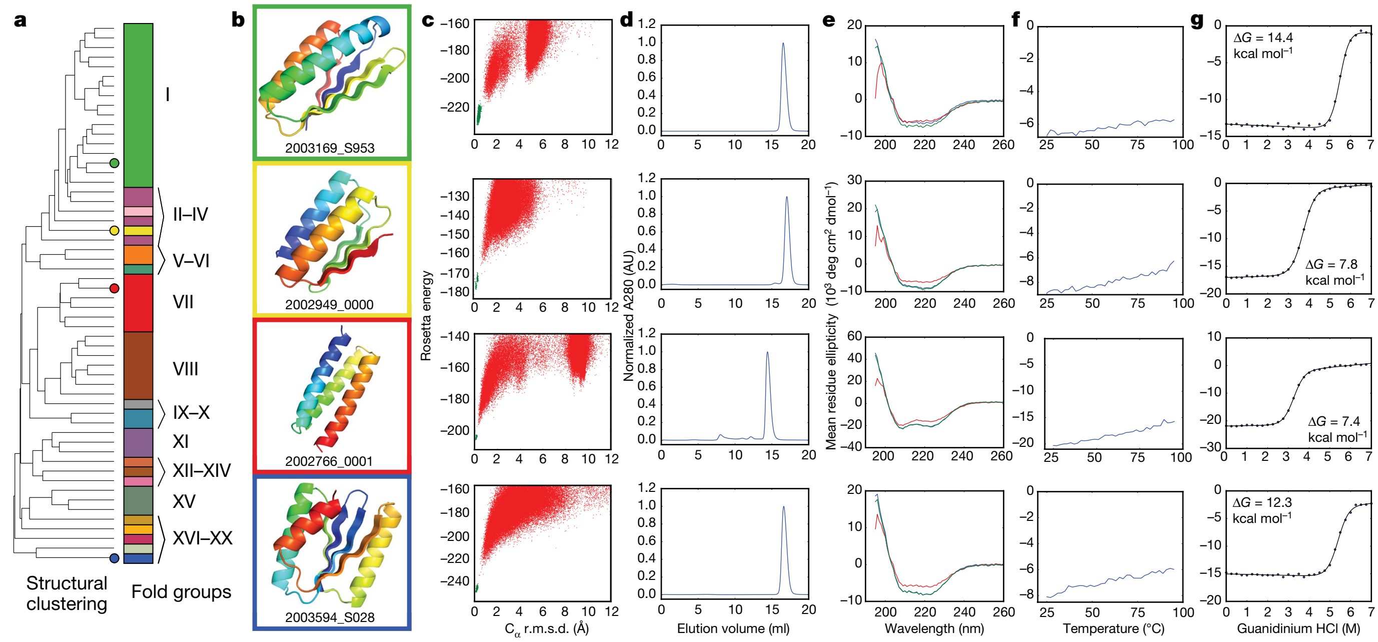

Fig. 3 | Structural characterization of Foldit player-designed proteins. **a**, Dendrogram showing all 56 folded Foldit player designs clustered by structural similarity (TM-align[26]), with coloured circles highlighting the four designs characterized in **b**–**g**. The stacked bars show the 20 different folds among the clustered designs (Extended Data Fig. 5). Fold XX (see design 2003594_S028) is a new fold, previously unobserved in natural proteins. **b**–**g**, Cartoon depiction of four select Foldit designs (**b**); the graphs in **c**–**g** correspond to these four structures. **c**, Rosetta@home ab initio calculations show that the sequence for each design has an energy landscape that is strongly funnelled towards the design structure. *y* axis, Rosetta energy; *x* axis, C_α r.m.s.d. to the designed structure; points represent lowest-energy structures sampled starting from an extended chain (red points) and starting from the Foldit design model (green points). **d**, Size-exclusion chromatography traces (absorbance at 280 nm) show that designs are monomeric in solution. **e**, Circular dichroism spectra indicate that the designs adopt the expected secondary structure content in solution at 25 °C (blue trace), when heated to 95 °C (red trace) and when cooled again to 25 °C (green trace). **f**, Circular dichroism mean residue ellipticity at 220 nm as temperature is increased from 25 °C to 95 °C; the designs do not denature with increasing temperature. **g**, Cooperative unfolding during titration with guanidinium hydrochloride. Blue circles show circular dichroism mean residue ellipticity at 220 nm with increasing concentration of denaturant, and the black curve shows a two-state unfolding model fit to the data. Free energy of unfolding (ΔG_{unf}) was determined by linear extrapolation using the fit model parameters[27].

We obtained custom synthetic genes encoding 12 player designs for which structure prediction calculations converged on the player-designed conformation[17]. The sequences of these proteins have no homology to any known protein (Supplementary Table 1). The de novo designs were expressed in *E. coli* and purified by metal-affinity and size-exclusion chromatography. Analysis by chromatography and circular dichroism indicated that 6 of the 12 designs were monomeric and folded in solution, with helical secondary structure consistent with the players' models (Supplementary Fig. 1). All of the experimentally tested proteins described in this paper are entirely the work of Foldit players.

During gameplay, the Foldit application uploads the player's latest model to the Foldit server every 2–5 minutes; from these snapshots we can reconstruct the process by which a Foldit player develops a protein design (Fig. 2). Foldit players use more-varied and complex exploration strategies than standard Rosetta automated design protocols, and frequently revert to a previous iteration of their model to explore an alternative path, resulting in a highly branched search tree. A typical automated design protocol, by contrast, includes only two branch points[18]. In addition, Foldit players regularly sample much higher energy states than the automated protocol, which has only a limited ability to escape local energy minima.

Encouraged by the success of Foldit players in designing stable proteins from scratch, we made additions to the game to encourage players to explore more-diverse protein structures. Up until this point, all top-scoring Foldit designs had consisted of either three or four α-helices connected by minimal loops. Indeed, Foldit players had determined that designs with β-sheets did not score as well as α-helical bundles (Extended Data Fig. 2), and competitive players had abandoned any attempt to design more varied folds. This is an interesting parallel to protein design by practicing scientists, which has also focused much more on helical bundles than on other classes of protein folds[19–22]. To encourage the design of a wider variety of folds, we introduced a 'secondary structure' rule, stipulating that no more than 50% of residues may form α-helices. Foldit players responded by designing a multitude of mixed α/β-proteins, which were indistinguishable from expert designs on visual inspection. However, structure prediction calculations for these α/β design sequences showed poor sampling close to the target design structure, which suggests that the designed sequences did not strongly encode their local structures[17]. Further analysis showed that these player designs contained many residues with locally strained backbone conformations (backbone ϕ and ψ torsions in unfavoured regions of the Ramachandran plot[23,24]). That such designs had very low energies revealed a problem in the Rosetta energy function at the time: because Rosetta users typically sampled backbones starting from fragments of native proteins, unfavourable local conformations were rarely encountered—therefore, it had not been discovered that the energies associated with local-backbone strain were being underestimated. We addressed this flaw in the Rosetta model by increasing the steepness of the energetic penalties associated with strained local-backbone geometry; this is now implemented in the latest Rosetta energy function[11]. We also added to Foldit an 'ideal loops' rule that restricted players to a set of 19 unstrained reverse-turn conformations[7], and incorporated new tools to aid generation of unstrained backbones: a fragment lookup-based loop-closure tool, an interactive Ramachandran map and a protein blueprint scheme for drag-and-drop assembly of secondary structure elements and common loop conformations (Extended Data Fig. 3). Together, these upgrades brought about a marked improvement in the local-backbone quality of Foldit player-designed proteins (Extended Data Fig. 4).

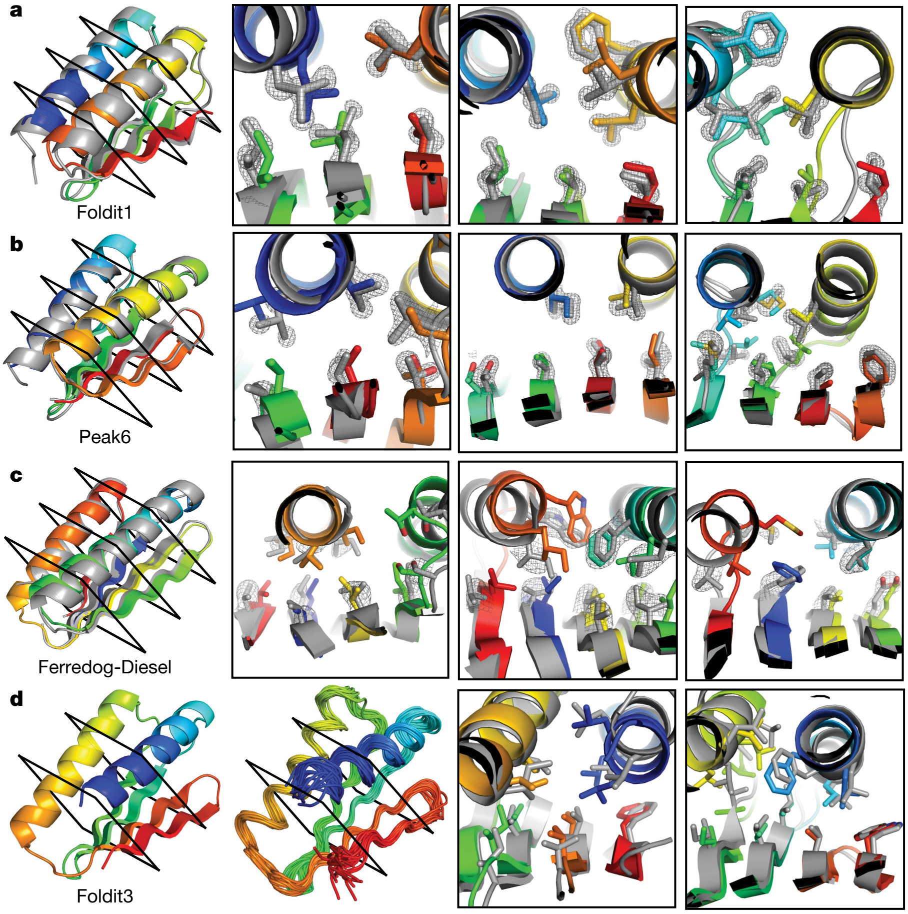

Fig. 4 | High-resolution structures of Foldit player-designed proteins. **a**, The Foldit1 design (fold V in Fig. 3: three β-strands with sheet order 1–2–3) model backbone (rainbow) aligns to the crystal structure (grey) with C_α r.m.s.d. of 1.1 Å. **b**, The Peak6 design (fold III: four strands, sheet order 1–2–4–3) model backbone aligns to the crystal structure with C_α r.m.s.d. of 0.9 Å. **c**, The Ferredog-Diesel design (fold I: four strands, sheet order 4–1–3–2) model backbone aligns to the crystal structure with C_α r.m.s.d. of 1.7 Å. Cross sections show core-residue sidechains, with the composite omit $2mF_o - DF_c$ map contoured at 2.0σ (**a**, **b**) or 1.0σ (**c**). **d**, The Foldit3 design model (fold XVII: four strands, sheet order 2–1–3–4) and NMR ensemble. The design model aligns to the representative (medoid) NMR model with a C_α r.m.s.d. of 1.1 Å. Cross sections compare core sidechains in the design model (rainbow) and representative NMR model (grey).

The importance of reducing local-backbone strain was borne out in experimental characterization. Before the backbone modelling improvements described in the previous paragraph, only 4 of 37 Foldit α/β-designs tested (11%) were monomeric and structured in solution. Following the backbone modelling additions, 46 of 97 (47%) were monomeric and exhibited the expected secondary structure in solution. Most showed exceptional stability in thermal and chemical denaturation experiments, with some free energies of unfolding (ΔG_{unf}) exceeding 20 kcal mol^{-1}; indeed, 32 designed proteins remained completely folded at 95 °C (Fig. 3, Supplementary Fig. 1). This success rate surpasses that in previous reports of designed α/β-proteins[7,12].

Overall, the 56 successful Foldit designs are diverse in structure, representing 20 different protein folds (Fig. 3, Extended Data Fig. 5), one of which is a new fold that is previously unobserved in natural proteins. The success of Foldit designs is not attributed to just one or two exceptional Foldit players, but is shared broadly by the Foldit community (Supplementary Table 1). The 56 successful designs were created by 36 different Foldit players (the most prolific player created 10 successful designs); 19 designs were created collaboratively by at least 2 cooperating players; and 5 successful designs were not top-scoring, but were nevertheless flagged by players as personal favourites. Foldit players lack formal expertise in protein modelling (Extended Data Fig. 6, Supplementary Notes), but knowledge and intuition gained from playing protein structure prediction puzzles in Foldit translated to success in de novo protein design (Extended Data Fig. 7).

We succeeded in solving high-resolution structures of four Foldit player-designed proteins. X-ray crystal structures of three designed proteins (named by their designers Foldit1, Peak6 and Ferredog-Diesel) closely match the designed conformations, with C_α root mean square deviations (r.m.s.d.) of 1.1, 0.9 and 1.7 Å, respectively (Fig. 4). Well-resolved electron density in the protein core of Foldit1 and Peak6 shows that most sidechains adopt the intended rotamers and preserve the designed packing interactions. The electron density of Ferredog-Diesel is less clear, but the protein backbone adopts the designed fold, and many core sidechains appear to pack as intended. The solution nuclear magnetic resonance (NMR) structure of a fourth design, Foldit3, also closely matches the design conformation, with a C_α r.m.s.d. of 1.1 Å between the design model and the medoid conformer[25] of the ensemble.

From these results, we can draw several general conclusions about scientific models, citizen science and the interplay between the two. First, a scientific model that holds within the domain space considered by practicing scientists may not hold outside of this domain. This is most vividly illustrated by the highly extended structures generated by Foldit players in their first de novo design efforts, and later by the structures with strained local geometry not previously sampled by Rosetta users. Second, for citizen scientists to make essential and creative scientific contributions through online gaming, the scoring function of the game must be an accurate representation of the science. In our initial iterations, Foldit did not present to players a sufficiently accurate and general model to allow them to robustly design new proteins, even though the underlying Rosetta software had been used for protein design by practicing scientists. Third and most importantly, citizen science offers a powerful way to systematically improve a scientific model through iterations of model trial and model improvement. Human game players are exceptionally capable at finding and exploiting unanticipated solutions that are otherwise unexplored by experienced scientists, whose focus is not on getting a high score, but rather on solving their specific scientific problem.

We have demonstrated that non-expert citizen scientists, playing the online computer game Foldit, can accurately design completely new protein structures from scratch. Locally, players' solutions are physically plausible and resemble natural proteins, but globally, they are creative and diverse. Proteins designed by citizen-scientist Foldit players are by no measure inferior to those of expert protein designers: they fold accurately to the intended conformation, show exceptional folding stability and span a wide diversity of structures. This result is all the more impressive given that de novo protein design was an almost completely unsolved problem just a few years ago, and the diversity in protein folds spanned by the successful Foldit players' models considerably exceeds that in any previous protein design report, to our knowledge. The sustained success of Foldit players over a wide diversity of protein folds highlights the power of human creativity when guided by scientific understanding presented in a readily comprehensible form.

Online content

Any methods, additional references, Nature Research reporting summaries, source data, statements of data availability and associated accession codes are available at https://doi.org/10.1038/s41586-019-1274-4.

Received: 19 October 2018; Accepted: 14 May 2019;
Published online 5 June 2019.

1. Lintott, C. J. et al. Galaxy Zoo: morphologies derived from visual inspection of galaxies from the Sloan Digital Sky Survey. *Mon. Not. R. Astron. Soc*. **389**, 1179–1189 (2008).
2. Kim, J. S. et al. Space-time wiring specificity supports direction selectivity in the retina. *Nature* **509**, 331–336 (2014).
3. Kawrykow, A. et al. Phylo: a citizen science approach for improving multiple sequence alignment. *PLoS ONE* **7**, e31362 (2012).
4. Lee, J. et al. RNA design rules from a massive open laboratory. *Proc. Natl Acad. Sci. USA* **111**, 2122–2127 (2014).
5. Cooper, S. et al. Predicting protein structures with a multiplayer online game. *Nature* **466**, 756–760 (2010).
6. Epstein, C. J., Goldberger, R. F. & Anfinsen, C. B. The genetic control of tertiary protein structure: studies with model systems. *Cold Spring Harb. Symp. Quant. Biol*. **28**, 439–449 (1963).
7. Lin, Y.-R. et al. Control over overall shape and size in de novo designed proteins. *Proc. Natl Acad. Sci. USA* **112**, E5478–E5485 (2015).
8. Huang, P.-S., Boyken, S. E. & Baker, D. The coming of age of *de novo* protein design. *Nature* **537**, 320–327 (2016).
9. Marcos, E. et al. Principles for designing proteins with cavities formed by curved β sheets. *Science* **355**, 201–206 (2017).
10. Dou, J. et al. De novo design of a fluorescence-activating β-barrel. *Nature* **561**, 485–491 (2018).
11. Alford, R. F. et al. The Rosetta all-atom energy function for macromolecular modeling and design. *J. Chem. Theory Comput*. **13**, 3031–3048 (2017).
12. Khatib, F. et al. Crystal structure of a monomeric retroviral protease solved by protein folding game players. *Nat. Struct. Mol. Biol*. **18**, 1175–1177 (2011).
13. Eiben, C. B. et al. Increased Diels–Alderase activity through backbone remodeling guided by Foldit players. *Nat. Biotechnol*. **30**, 190–192 (2012).
14. Blout, E. R. & Idelson, M. Compositional effects on the configuration of water-soluble polypeptide copolymers of l-glutamic acid and l–lysine. *J. Am. Chem. Soc*. **80**, 4909–4913 (1958).
15. Doty, P., Imahori, K. & Klemperer, E. The solution properties and configurations of a polyampholytic polypeptide: copoly-l-lysine-l-glutamic acid. *Proc. Natl Acad. Sci. USA* **44**, 424–431 (1958).
16. Ghosh, K. & Dill, K. A. Theory for protein folding cooperativity: helix bundles. *J. Am. Chem. Soc*. **131**, 2306–2312 (2009).
17. Rohl, C. A., Strauss, C. E. M., Misura, K. M. S. & Baker, D. Protein structure prediction using Rosetta. *Methods Enzymol*. **383**, 66–93 (2004).
18. Koga, N. et al. Principles for designing ideal protein structures. *Nature* **491**, 222–227 (2012).
19. Regan, L. & DeGrado, W. F. Characterization of a helical protein designed from first principles. *Science* **241**, 976–978 (1988).
20. Harbury, P. B., Plecs, J. J., Tidor, B., Alber, T. & Kim, P. S. High-resolution protein design with backbone freedom. *Science* **282**, 1462–1467 (1998).
21. Thomson, A. R. et al. Computational design of water-soluble α-helical barrels. *Science* **346**, 485–488 (2014).
22. Jacobs, T. M. et al. Design of structurally distinct proteins using strategies inspired by evolution. *Science* **352**, 687–690 (2016).
23. Ramachandran, G. N. & Sasisekharan, V. Conformation of polypeptides and proteins. *Adv. Protein Chem*. **23**, 283–438 (1968).
24. Chen, V. B. et al. MolProbity: all-atom structure validation for macromolecular crystallography. *Acta Crystallogr. D* **66**, 12–21 (2010).
25. Montelione, G. T. et al. Recommendations of the wwPDB NMR Validation Task Force. *Structure* **21**, 1563–1570 (2013).
26. Zhang, Y. & Skolnick, J. TM-align: a protein structure alignment algorithm based on the TM-score. *Nucleic Acids Res*. **33**, 2302–2309 (2005).
27. Santoro, M. M. & Bolen, D. W. Unfolding free energy changes determined by the linear extrapolation method. 1. Unfolding of phenylmethanesulfonyl α-chymotrypsin using different denaturants. *Biochemistry* **27**, 8063–8068 (1988).

Acknowledgements We thank all Foldit players for their gameplay contributions, and for feedback offered on the Foldit website (https://fold.it). We thank A. Kang, S. A. Rettie, C. Chow and L. Carter for help with experiments; D. Alonso, L. Goldschmidt, P. Vecchiato and D. Kim for computer support; and Rosetta@home (https://boinc.bakerlab.org) volunteers for computing resources. We thank G. Rocklin, V. Mulligan and other members of the Baker laboratory for discussions. This material is based on work supported by the National Science Foundation (NSF) Graduate Research Fellowship under grant no. DGE-1256082, NSF grant no. 1629879, National Institutes of Health (NIH) grant 1UH2CA203780, and NIH grants 1S10 OD018207 and 5R01 GM120574 (to G.T.M.) and HHMI (D.B.). The ALS-ENABLE beamlines are supported in part by the NIH, National Institute of General Medical Sciences, grant P30 GM124169-01. The Advanced Light Source is a DOE User Facility under contract no. DE-AC02-05CH11231. Foldit3 was a nominated target of the CASP COMMONS Community Outreach program.

Reviewer information *Nature* thanks Jérôme Waldispuhl and the other anonymous reviewer(s) for their contribution to the peer review of this work.

Author contributions B.K., Z.P., F.K., S.C. and D.B. designed the study. B.K., J.F., T.H., A.F., D.-A.S. and S.C. developed Foldit software tools. A. Boykov, R.D.E., S.K., T.N.-S. and L.W., along with the other Foldit players, designed all proteins. B.K., F.K., A.F. and A. Bauer analysed Foldit player designs. B.K. performed biophysical characterization. B.K., M.J.B. and F.D. determined crystal structures. G.L., Y.I. and G.T.M. determined the NMR structure. B.K. and D.B. wrote the manuscript with input from all authors. Foldit players contributed extensively through their feedback and gameplay, which generated the data for this paper.

Competing interests G.T.M. is a co-founder of Nexomics Biosciences.

Additional information
Extended data is available for this paper at https://doi.org/10.1038/s41586-019-1274-4.
Supplementary information is available for this paper at https://doi.org/10.1038/s41586-019-1274-4.
Reprints and permissions information is available at http://www.nature.com/reprints.
Correspondence and requests for materials should be addressed to D.B.
Publisher's note: Springer Nature remains neutral with regard to jurisdictional claims in published maps and institutional affiliations.

METHODS

Foldit protein design puzzles. Foldit puzzles were set up with a model polyisoleucine in fully extended conformation, with fixed length ranging from 60 to 100 residues. Each puzzle was posted online for seven days, during which Foldit players competed to develop a protein model with the lowest energy, as calculated by the Rosetta energy function. Foldit puzzles used the talaris2013_cart scorefunction with the following modifications: (1) the cart_bonded scoreterm was upweighted (increased from 0.5 to 2.0) to ensure realistic bond lengths and angles as players cut and splice the backbone chain; (2) a penalty-only envsmooth scoreterm (weighted at 2.0) was added to supplement the Rosetta solvation treatment, and to discourage the design of buried polar and exposed nonpolar residues; (3) the reference energy of alanine was modified (increased to 3.0) to discourage the excessive design of alanine. Configuration files for all Foldit puzzles are provided in the Supplementary Data. Each Foldit puzzle was accompanied by a brief description, along with an explanation of any supplementary rules enforced in the puzzle. Design puzzles were accessible to all Foldit users; Foldit user registration is free and open to the public, at http://fold.it. Models were collected continuously as Foldit players worked on the puzzles, as the Foldit application automatically uploads the user's latest model to a server every 2–5 min. This study was approved by the University of Washington Institutional Review Board, and informed consent for this research was obtained from all Foldit users at the time of user registration.

Protein design selection. After the end of each puzzle, we selected player models for further analysis as follows: first, we selected the lowest-energy model from each of the ten top-ranked groups, in which independent players were treated as individual groups (designs named with suffix '0000-9'). Second, we selected the lowest-energy model from the ten top-ranked solo players, which includes independent players as well as group members that developed a model without assistance from their group (suffix 's000-9'). Third, we visually inspected models that were flagged by Foldit players for special consideration, and selected any models that appeared plausible (suffix 'S***'). Last, we ranked and pruned the set of remaining models by removing any models that align to a better-scoring model with C_α r.m.s.d. less than 2.5 Å. We visually inspected the 50 top-ranked models in the pruned set and selected any models that appeared plausible (suffix '1001-50'). Models deemed 'implausible' typically lacked secondary structure, contained buried polar residues or included long stretches of completely polar residues. At each step, we used TM-align[26] to eliminate duplicate models (TM-score >0.98) that had already been selected (for example, models that were top-ranking and flagged by players). In rounds 2 and 3, the top-ranked group and solo models were automatically selected for further analysis, without visual inspection. The sequences of selected models were subjected to Rosetta ab initio structure prediction[17], using the distributed computing platform Rosetta@home. If ab initio predictions identified any decoy structures with energy comparable to (or lower than) the designed structure, or if ab initio predictions were unable to sample the designed structure, the design was rejected. All other designs were selected for experimental characterization. See Extended Data Table 1 for summary statistics on design selection. The majority of experimentally tested designs (96 of 146) were top-ranked group or solo designs, which were selected 'blindly' (without visual inspection). Models and FASTA sequences of all tested designs are shown in the Supplementary Data.

Protein expression and purification. A 6×His tag with TEV-cleavable linker (sequence MGHHHHHHGWSENLYFQGS) was prepended to the N terminus of each design selected for experimental characterization. Plasmids containing the encoded genes were ordered from Genscript in pET15 (designs with prefix between 997258 and 1998925), in pET21 (1998555–2002990) or from Twist in pET29 (2003048-2003594) vectors. Plasmids were transformed into *E. coli* BL21 Star (DE3) cells (Invitrogen), and grown overnight in 4 ml Luria–Bertani (LB) medium with 50 μg/ml carbenicillin (for pET15, pET21 vectors) or 30 μg/ml kanamycin (for pET29). Overnight cultures were used to inoculate 0.5 l auto-induction medium, and grown at 37 °C for 18 h. Cultures were pelleted and resuspended in 25 ml lysis buffer (20 mM Tris pH 8.0, 300 mM NaCl, 1 mg/ml lysozyme, 0.1 mg/ml DNase, 1 mM PMSF), and lysed by microfluidization. The cell lysate was pelleted and supernatant was filtered with a 0.22-μm filter before loading onto a 2 ml nickel-affinity gravity column. Protein bound to the column was washed with 20 ml wash buffer (20 mM Tris pH 8.0, 500 mM NaCl, 30 mM imidazole) and eluted in 10 ml elution buffer (20 mM Tris pH 8.0, 500 mM NaCl, 250 mM imidazole). Purified protein was dialysed into TBS (20 mM Tris pH 8.0, 300 mM NaCl) at 4 °C overnight to remove imidazole and further purified by size-exclusion chromatography on an AKTAxpress (GE Healthcare) with a Superdex S75 10/300 GL column (GE Healthcare). For proteins containing cysteine, dialysis and gel filtration were carried out in TBS with 1 mM tris(2-carboxyethyl)phosphine (TCEP). Protein expression and solubility was determined from SDS–PAGE and mass spectrometry. Oligomeric state was determined by size-exclusion chromatography.

Circular dichroism. Purified protein was dialysed into 50 mM sodium phosphate pH 7.4 at 4 °C overnight (plus 500 μM TCEP for proteins containing cysteine). All circular dichroism data were collected on an AVIV Model 420 spectrometer. Far UV spectra and temperature melts were measured with 11–62 μM protein in a quartz cuvette with path length of 1 mm. Protein concentration was determined by absorbance at 280 nm using a NanoDrop spectrophotometer (Thermo Scientific), using predicted extinction coefficients. Wavelength spectra were measured between 195 and 260 nm at 25 °C, 95 °C and again after cooling to 25 °C. For temperature melts, ellipticity at 220 nm was monitored as temperature increased from 25 °C to 95 °C in increments of 2 °C. Chemical titrations were carried out with 1.0–21 μM protein in a quartz cuvette with path length of 10 mm. Ellipticity at 220 nm was monitored at concentrations of guanidinium chloride increasing from 0 to 7 M, in increments of 0.25 M. Denaturation curves were fitted with nonlinear regression to two-state unfolding model with six parameters: the folding free energy, *m*-value, and slope and *y* intercept for baseline curves[27].

X-ray crystallography. Prior to X-ray crystallography, the N-terminal 6×His tag was cleaved from protein samples by incubation with 250 μg TEV protease at 25 °C for 4 h in 20 mM Tris pH 8.0, 300 mM NaCl, 1 mM DTT. The reaction product was dialysed into TBS overnight at 4 °C to remove DTT and flowed over a 2 ml metal-affinity gravity column to remove TEV protease and residual histidine tag. The cleaved protein was further purified by gel filtration as described above. Purified protein was concentrated to 20–100 mg/ml in 20 mM Tris pH 8.0, 300 mM NaCl. Crystallization screening was carried out with a variety of 96-condition spare matrix suites available from Qiagen or Hampton Research. A Mosquito Crystal nanolitre robot (TTP Labtech) was used to prepare screens in 3-well sitting drop plates, with 200 nl drops and protein:precipitant ratios of 1:1, 1:2 and 2:1.

Foldit1 (2002949_0000) was crystallized at 20 mg/ml in 50 mM HEPES pH 7.5, 0.2 M potassium chloride, 35% v/v pentaerythritol propoxylate. Crystals were flash-frozen in liquid nitrogen without further cryo-protection. X-ray diffraction was collected to a resolution of 1.18 Å.

Peak6 (2003333_0006) was crystallized at 40 mg/ml in 0.1 M sodium acetate pH 4.5, 0.2 M lithium sulphate, 50% w/v PEG 400. Crystals were briefly soaked in mother liquor plus 20% PEG 200, then flash-frozen in liquid nitrogen. X-ray diffraction was collected to a resolution of 1.54 Å.

Ferredog-Diesel (2003169_S953) was crystallized with 6×His tag intact, at 80 mg/ml in 0.1 M citrate pH 4.0, 3.0 M NaCl. Crystals were dehydrated by soaking in 5 μl mother liquor in open air for 10 min, then flash-frozen in liquid nitrogen. X-ray diffraction was collected to a resolution of 1.92 Å.

X-ray diffraction datasets were collected at the Advanced Light Source (Berkeley, CA). Data was processed with HKL2000[28]. Crystal structures were solved by molecular replacement with Phaser[29], using the backbone of the original designed model with sidechains truncated to the β-carbon (Foldit1 and Peak6), or using the backbone of a model predicted ab initio from the design sequence (Ferredog-Diesel). Models were built and refined in iterative cycles using Coot and PHENIX[30,31]. Diffraction data and refinement statistics are listed in Extended Data Table 2.

NMR spectroscopy. NMR studies were performed using uniformly ^{15}N,^{13}C-enriched protein samples. A synthetic gene for Foldit3 (2003265_s008) was obtained from Genscript already incorporated into plasmid pET15TEV_NESG, which includes a N-terminal 6×His purification tag, followed by a TEV protease cleavage site (sequence MGHHHHHHGWSENLYFQGS). *E. coli* BL21(DE3) cells containing plasmid pET15TEV_NESG-Foldit3 were grown in 1 l MJ9 minimal medium[32], supplemented with 100 μg/ml ampicillin at 37 °C. To produce uniformly ^{15}N and ^{13}C-enriched protein samples, 1 g/l ^{15}NH$_4$ salts and 2g/l U-^{13}C glucose were added as sole nitrogen and carbon sources, respectively. When OD$_{600}$ reached around 0.5 units, the culture was transferred to 18 °C, and protein production was induced by addition of 1 mM IPTG. After overnight incubation, the cells were collected and resuspended in 20 ml binding buffer (20 mM Tris-HCl pH 8.0, 500 mM NaCl and 20 mM imidazole). After passing the cells through 900–1000 psi French press twice, cell debris were removed by 10,000 r.p.m. for 30 min. The supernatant was further spun down at 40,000 r.p.m. for 1 h. The obtained supernatant (soluble fraction) was mixed with 1 ml of Ni-resin and incubated at 4 °C for 1 h. The non-specific binding proteins were removed by 20 ml binding buffer and washing buffer (20 mM Tris-HCl pH 8.0, 500 mM NaCl and 50 mM imidazole) and the target protein was eluted by 5 ml elution buffer (20 mM Tris-HCl pH 8.0, 500 mM NaCl and 300 mM imidazole). The protein was dialysed against GF buffer (20 mM Tris-HCl pH 8.0, 100 mM NaCl) for overnight and gel filtration was carried out using AKTA express with high-load 26/600 Superdex 200 pg column. Homogeneity (>97%) was validated by SDS polyacrylamide gel electrophoresis. The purified protein was dialysed against 20 mM potassium phosphate (pH 6.5), and the protein concentration was adjusted to between 0.3–0.4 mM for NMR studies.

All NMR spectra were recorded at 25 °C using cryogenic NMR probes. All NMR data were collected on the Bruker AVANCE III 600 MHz spectrometers and processed using the program NMRPipe[33], and analysed using the programs SPARKY and XEASY[34]. Spectra were referenced to external DSS. Sequence-specific resonance assignments were determined using AutoAssign software together with interactive manual analysis, as previously described[35]. Backbone dihedral angle constraints were derived from the chemical shifts using the program TALOS_N[36] for residues located in well-defined secondary structure elements. The programs ASDP[37] and CYANA[38,39] were used to automatically assign NOEs and to calculate structures. RPF analysis[37,40] was used in parallel to guide iterative cycles of noise and artefact peak removal, peak picking, and NOESY peak assignments. The 20 conformers with the lowest target CYANA function value were then refined in explicit water[41] using the program CNS[42]. The structural statistics and global structure quality factors (Extended Data Table 3) including Verify3D[43], ProsaII[44], PROCHECK[45], and MolProbity[46] raw and statistical *Z*-scores were computed using the PSVS[47] v.1.5 and PDBStat[48] software packages. The global goodness-of-fit of the final structure ensembles with the NOESY peak list data, the NMR DP score, was determined using the RPF analysis program[40].

Reporting summary. Further information on research design is available in the Nature Research Reporting Summary linked to this paper.

Data availability

The atomic coordinates of Foldit1, Peak6 and Ferredog-Diesel crystal structures and the Foldit3 NMR structure have been deposited in the RCSB Protein Data Bank (PDB) with accession numbers 6MRR, 6MRS, 6NUK and 6MSP, respectively. Chemical shift and NOESY peak list data for Foldit3 were deposited in the Biological Magnetic Resonance Data Bank with accession number 30527.

Code availability

Because Foldit crowdsourcing relies on regulated, fair competition between participants, the source code of the Foldit user interface is not open. The underlying Rosetta macromolecular modelling suite (https://www.rosettacommons.org) is freely available to academic and non-commercial users, and commercial licenses are available via the University of Washington CoMotion Express License Program. Analysis scripts used in this paper are available in the Supplementary Information.

28. Otwinowski, Z. & Minor, W. Processing of X-ray diffraction data collected in oscillation mode. *Methods Enzymol.* **276**, 307–326 (1997).
29. McCoy, A. J. et al. Phaser crystallographic software. *J. Appl. Crystallogr.* **40**, 658–674 (2007).
30. Emsley, P., Lohkamp, B., Scott, W. G. & Cowtan, K. Features and development of Coot. *Acta Crystallogr. D* **66**, 486–501 (2010).
31. Afonine, P. V. et al. Towards automated crystallographic structure refinement with phenix.refine. *Acta Crystallogr. D* **68**, 352–367 (2012).
32. Jansson, M. et al. High-level production of uniformly ^{15}N- and ^{13}C-enriched fusion proteins in *Escherichia coli*. *J. Biomol. NMR* **7**, 131–141 (1996).
33. Delaglio, F. et al. NMRPipe: a multidimensional spectral processing system based on UNIX pipes. *J. Biomol. NMR* **6**, 277–293 (1995).
34. Bartels, C., Xia, T. H., Billeter, M., Güntert, P. & Wüthrich, K. The program XEASY for computer-supported NMR spectral analysis of biological macromolecules. *J. Biomol. NMR* **6**, 1–10 (1995).
35. Liu, G. et al. NMR data collection and analysis protocol for high-throughput protein structure determination. *Proc. Natl Acad. Sci. USA* **102**, 10487–10492 (2005).
36. Shen, Y., Delaglio, F., Cornilescu, G. & Bax, A. TALOS+: a hybrid method for predicting protein backbone torsion angles from NMR chemical shifts. *J. Biomol. NMR* **44**, 213–223 (2009).
37. Huang, Y. J., Tejero, R., Powers, R. & Montelione, G. T. A topology-constrained distance network algorithm for protein structure determination from NOESY data. *Proteins* **62**, 587–603 (2006).
38. Güntert, P., Mumenthaler, C. & Wüthrich, K. Torsion angle dynamics for NMR structure calculation with the new program DYANA. *J. Mol. Biol.* **273**, 283–298 (1997).
39. Herrmann, T., Güntert, P. & Wüthrich, K. Protein NMR structure determination with automated NOE assignment using the new software CANDID and the torsion angle dynamics algorithm DYANA. *J. Mol. Biol.* **319**, 209–227 (2002).
40. Huang, Y. J., Powers, R. & Montelione, G. T. Protein NMR recall, precision, and *F*-measure scores (RPF scores): structure quality assessment measures based on information retrieval statistics. *J. Am. Chem. Soc.* **127**, 1665–1674 (2005).
41. Linge, J. P., Williams, M. A., Spronk, C. A., Bonvin, A. M. & Nilges, M. Refinement of protein structures in explicit solvent. *Proteins* **50**, 496–506 (2003).
42. Brünger, A. T. et al. Crystallography & NMR system: a new software suite for macromolecular structure determination. *Acta Crystallogr. D* **54**, 905–921 (1998).
43. Lüthy, R., Bowie, J. U. & Eisenberg, D. Assessment of protein models with three-dimensional profiles. *Nature* **356**, 83–85 (1992).
44. Sippl, M. J. Recognition of errors in three-dimensional structures of proteins. *Proteins* **17**, 355–362 (1993).
45. Laskowski, R. A., Macarthur, M. W., Moss, D. S. & Thornton, J. M. Procheck—a program to check the stereochemical quality of protein structures. *J. Appl. Crystallogr.* **26**, 283–291 (1993).
46. Word, J. M., Bateman, R. C., Jr, Presley, B. K., Lovell, S. C. & Richardson, D. C. Exploring steric constraints on protein mutations using MAGE/PROBE. *Protein Sci.* **9**, 2251–2259 (2000).
47. Bhattacharya, A., Tejero, R. & Montelione, G. T. Evaluating protein structures determined by structural genomics consortia. *Proteins* **66**, 778–795 (2007).
48. Tejero, R., Snyder, D., Mao, B., Aramini, J. M. & Montelione, G. T. PDBStat: a universal restraint converter and restraint analysis software package for protein NMR. *J. Biomol. NMR* **56**, 337–351 (2013).
49. Trifonov, E. N. in *Structure and Methods, Vol. 1: The Proceedings of the Sixth Conversation held at The University–SUNY* (Adenine, 1990).
50. Holm, L. & Laakso, L. M. Dali server update. *Nucleic Acids Res.* **44** (W1), W351–W355 (2016).

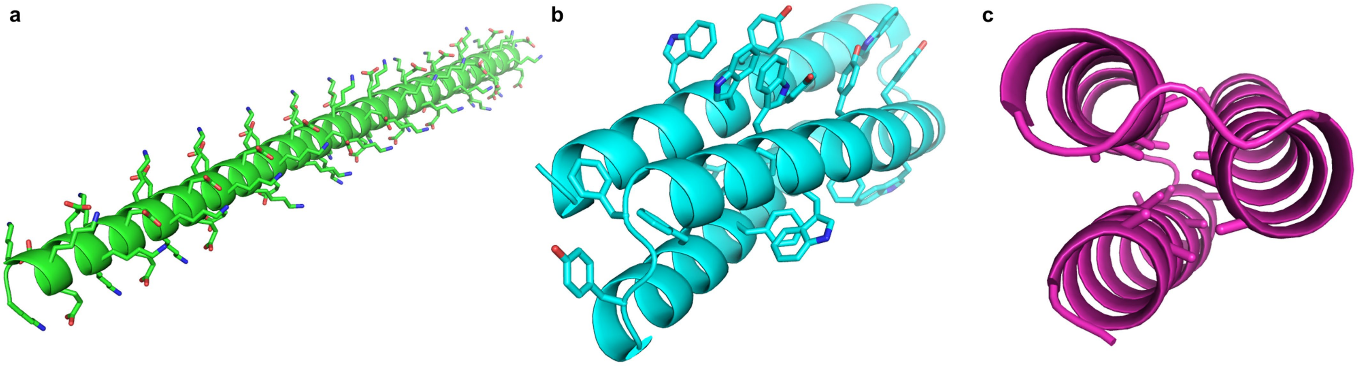

Extended Data Fig. 1 | Initial top-ranking Foldit player designs. When challenged to design a protein with only the talaris2013 score function (and no additional rules), Foldit players discovered low-energy models that are unlikely to fold as designed. **a**, An extended α-helix, composed entirely of lysine and glutamate, has very favourable energies for hydrogen-bonding, electrostatic and backbone torsions, but is unlikely to fold cooperatively into a single stable structure. This type of design is discouraged with the 'core exists' rule. **b**, Owing to their greater surface area, large aromatic sidechains can make more interactions than smaller aliphatic sidechains, even when underpacked or solvent-exposed. This type of design is discouraged with the 'residue interaction energy' rule. **c**, A design with an alanine- and glycine-saturated core can make favourable van der Waals interactions between closely packed backbone atoms; however, the burial of these small sidechains is associated with a weaker hydrophobic effect, and the lack of interdigitation allows exchange between multiple conformations with similar core packing energies (that is, molten globule behaviour). These designs are discouraged with the 'secondary structure design' rule.

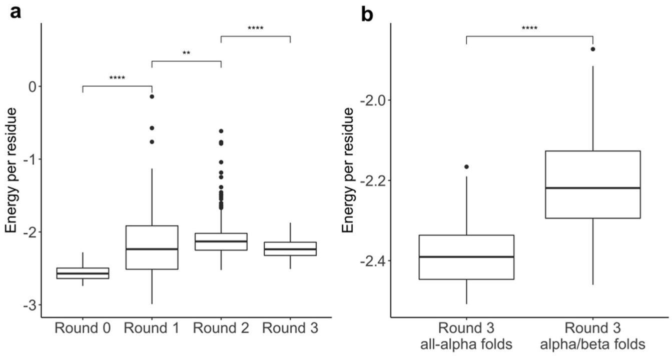

Extended Data Fig. 2 | Rosetta energy of top Foldit player designs. Rosetta energy of top-ranking designs was calculated with the talaris2013 score function and normalized by residue count. **a**, Energy of top-ten-ranked designs from: initial Foldit puzzles (round 0; $n = 30$ designs), round 1 puzzles ($n = 170$), round 2 puzzles ($n = 510$) and round 3 puzzles ($n = 250$). The introduction of supplementary rules in round 1 and round 2 resulted in higher-energy designs ($P < 10^{-6}$ and $P < 0.01$, respectively; Wilcoxon rank-sum test). The backbone modelling improvements in round 3 resulted in lower-energy designs ($P < 10^{-15}$; Wilcoxon rank-sum test). **b**, Energy of top-ten-ranked designs from round three all-α puzzles ($n = 30$) or α/β-puzzles using the 'secondary structure' rule ($n = 220$). All-α designs tend to have lower energy than α/β-designs ($P < 10^{-10}$; Wilcoxon rank-sum test). Box plots show: centre line, median; box limits, upper and lower quartiles; whiskers, 1.5× interquartile range; points, outliers.

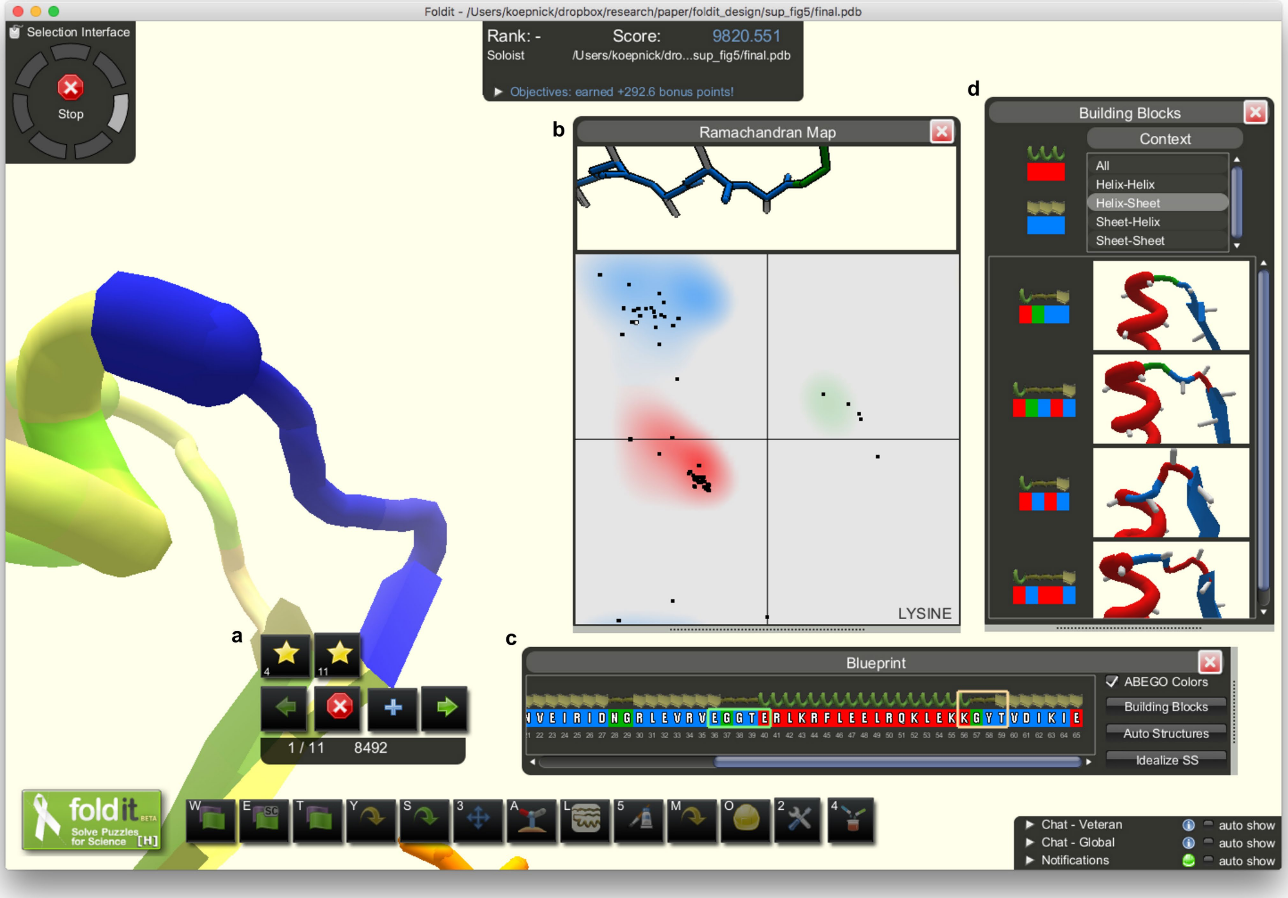

Foldit - /Users/koepnick/dropbox/research/paper/foldit_design/sup_fig5/final.pdb

Rank: - Score: 9820.551
Soloist /Users/koepnick/dro...sup_fig5/final.pdb

▶ Objectives: earned +292.6 bonus points!

Extended Data Fig. 3 | New backbone-modelling tools in Foldit. **a**, The ‘remix’ tool allows players to select a region of the model and search a library of backbone fragments for a conformation that can be substituted. **b**, An interactive Ramachandran map allows players to easily identify residues with outlier backbone conformations. Players can also click and drag points on the Ramachandran map to set the backbone torsions of individual residues. **c**, A ‘blueprint’ panel shows the primary sequence and secondary structure content of the model. Residues are coloured according to the ABEGO quadrants of the Ramachandran plot[7]. **d**, Players can drag-and-drop modular building blocks onto the blueprint panel to insert common turn conformations into their model.

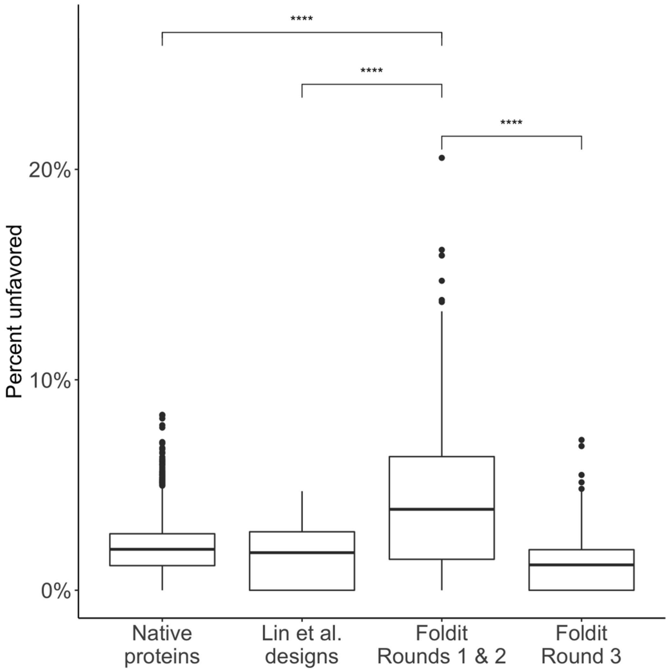

Extended Data Fig. 4 | Improvement of backbone quality in round 3 Foldit designs. MolProbity[24] was used to calculate the proportion of residues with unfavored or outlier backbone torsions in: high-resolution crystal structures of native proteins ($n = 6{,}342$), de novo design models from a previous study[7] ($n = 72$), and top-ranking Foldit player designs from before ($n = 680$) and after ($n = 250$) improvements to Foldit backbone-modelling tools. Initial Foldit player designs contained significantly more unfavoured torsions than native proteins or other de novo designs from a previous study[7] ($P < 10^{-15}$, two-tailed *t*-test). Improvements to Foldit's backbone-modelling tools led Foldit players to produce designs with fewer unfavoured torsions ($P < 10^{-15}$, two-tailed *t*-test). Box plots show: centre line, median; box limits, upper and lower quartiles; whiskers, 1.5× interquartile range; points, outliers.

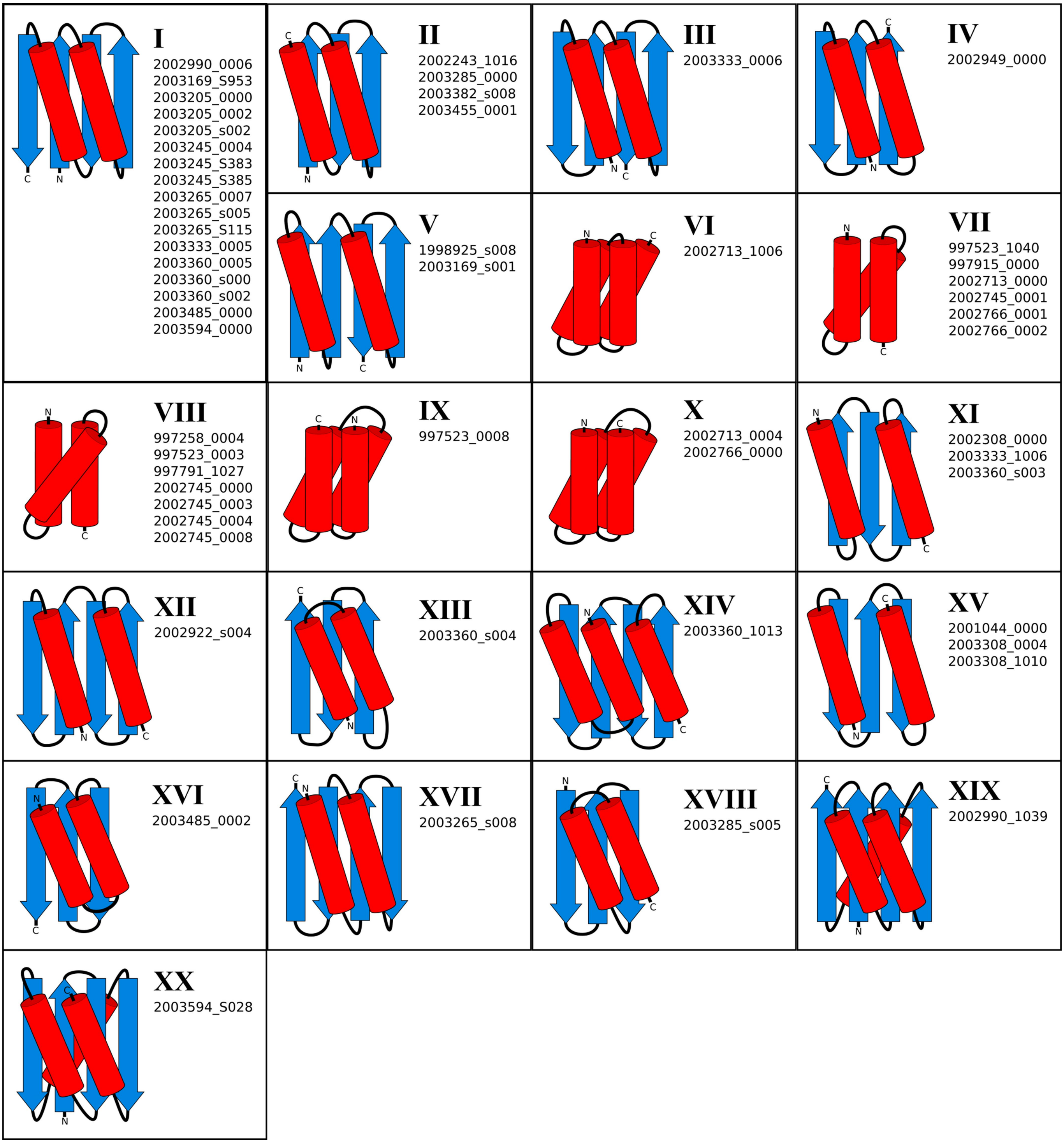

Extended Data Fig. 5 | Protein folds represented by successful Foldit player designs. Each fold has a unique arrangement and connectivity of secondary structure elements, depicted in cartoon diagrams. Diagrams are labelled with Roman numerals as in Fig. 3. Fold XX is a new fold, previously unobserved in natural proteins; TM-align[26] and DALI[50] alignments of design 2003594_S028 against the entire PDB found no structural homologues with this fold.

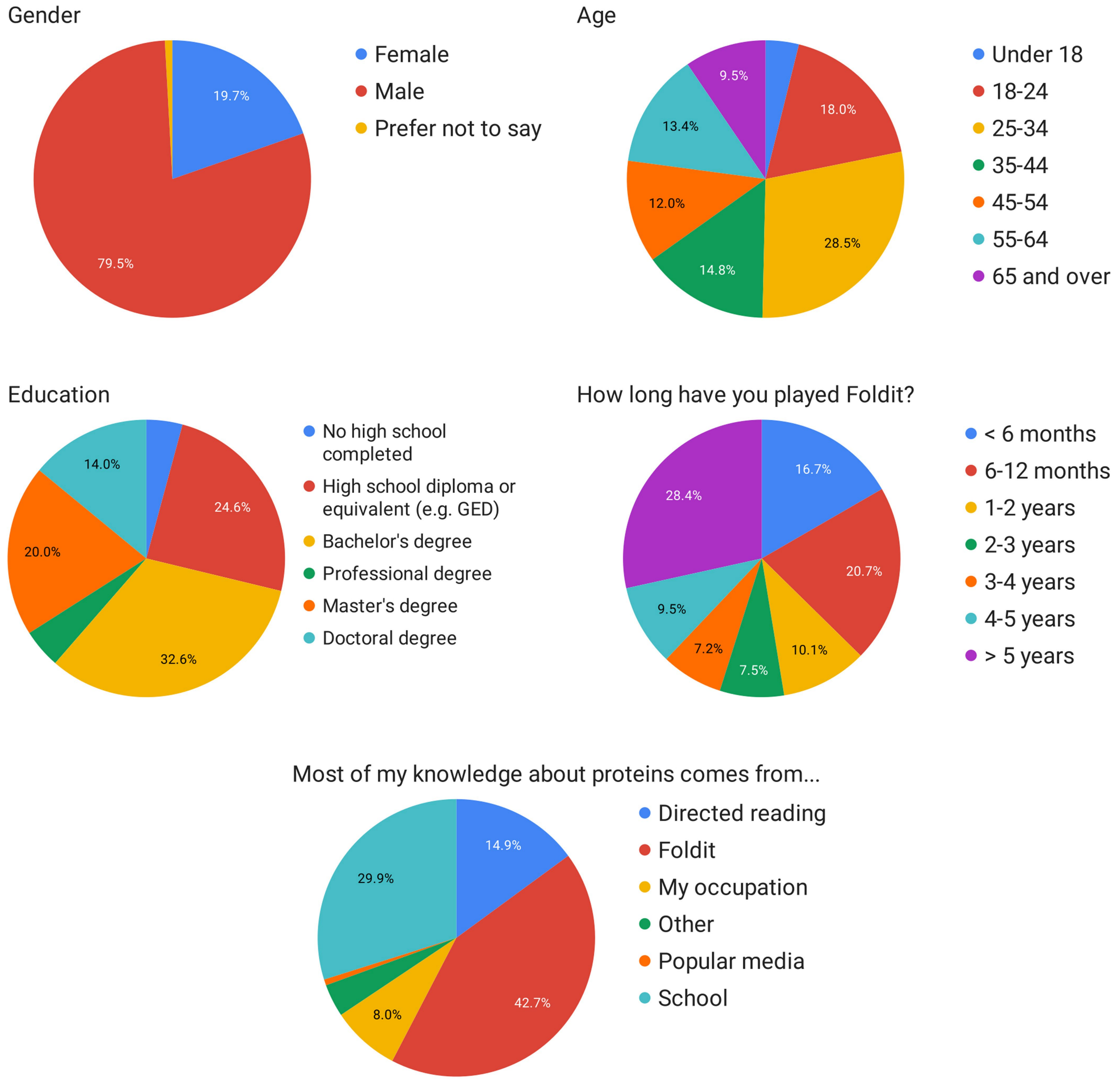

Extended Data Fig. 6 | Foldit player demographics. All players who participated in Foldit protein design puzzles and who had not opted out of Foldit-related email were solicited for survey questions. Data are shown for $n = 324$ responding Foldit players.

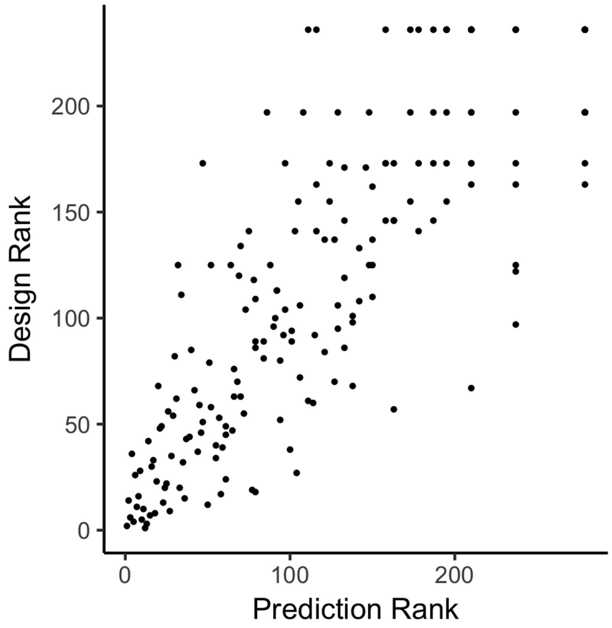

Extended Data Fig. 7 | Category rankings of Foldit players. Foldit player rankings are strongly correlated in the design and prediction categories (Spearman's rank correlation coefficient of 0.84). This suggests that skills developed playing Foldit structure prediction puzzles carry over to design puzzles and vice versa.

Extended Data Table 1 | Success rates of Foldit player-designed proteins

	Foldit player designs									
	Round 0		Round 1		Round 2		Round 3		Lin et al.[7]	
Sequence complexity*	0.20		0.35		0.44		0.21		0.20	
Rosetta energy† (per residue)	-2.6	± 0.1	-2.2	± 0.5	-2.1	± 0.2	-2.2	± 0.1	-1.9	± 0.1
Total puzzles	3		17		51		25			
Avg. players per puzzle	123	± 19	212	± 34	189	± 36	151	± 16		
Raw model count	140,273		2,887,213		10,556,093		4,124,471			
Top models	60		340		1020		500			
Shared models	53		214		726		342			
Clustered models	150		850		2550		1250			
Total models considered‡	263		1404		4296		2092			
Models selected for ab initio	0		100		1141		612		*(Not reported)*	
Ab initio convergence	NA		12	12%	37	3%	99	16%	72	
Models tested	NA		12		37		97		72	
Expressed	NA		12	100%	23	62%	86	89%	70	97%
… and soluble	NA		12	100%	18	49%	71	73%	64	89%
… and monomeric	NA		7	58%	7	19%	52	54%	39	54%
… and structured	NA		6	50%	4	11%	46	47%	29	40%
Number of unique folds	NA		3		4		19		2	

*Linguistic sequence complexity[49] was calculated from the top-ten-ranked models in all puzzles, using word lengths of 1, 2 and 3.

†Rosetta energy is the talaris2013 energy normalized by residue count. Values shown are mean and standard deviation for the ten top-ranked models in all puzzles. See Extended Data Fig. 2 for sample sizes.

‡Includes redundant models, as very similar models can appear in two or more categories (top, shared and clustered). See Methods for details on model selection.

Extended Data Table 2 | X-ray crystallography data and refinement statistics

	Foldit1 (6MRR)	Peak6 (6MRS)	Ferredog-Diesel (6NUK)
Data collection			
Space group	P 1 2_1 1	P 3_1 2 1	P 4_2 2_1 2
Cell dimensions			
a, *b*, *c* (Å)	24.05, 43.58, 29.28	52.41, 52.41, 56.09	69.21, 69.21, 90.59
α, β, γ (°)	90, 99.0, 90	90, 90, 120	90, 90, 90
Resolution (Å)	28.92 - 1.18 (1.222 - 1.18)	26.21 - 1.541 (1.596 - 1.541)	45.29 - 1.916 (1.985 - 1.916)
R_{merge}	0.02508 (0.1209)	0.0872 (0.7896)	0.08947 (3.164)
$I / \sigma I$	25.65 (9.97)	18.52 (1.34)	16.94 (0.86)
Completeness (%)	92.67 (88.38)	94.86 (65.00)	99.06 (97.65)
Redundancy	3.3 (3.4)	10.1 (4.8)	11.7 (11.5)
Refinement			
Resolution (Å)	1.18	1.541	1.916
No. reflections	18574	12861	17376
R_{work} / R_{free}	0.146 / 0.182	0.168 / 0.198	0.248 / 0.291
No. atoms			
Protein	574	646	1672
Ligand/ion	0	20	0
Water	116	89	37
B-factors			
Protein	14.54	22.82	69.09
Ligand/ion	0	47.36	0
Water	25.39	35.49	55.90
R.m.s. deviations			
Bond lengths (Å)	0.008	0.007	0.005
Bond angles (°)	0.83	1.03	1.01

Values in parentheses are for highest resolution shell. X-ray diffraction data for each protein structure were collected on a single crystal and processed as described in the Methods.

Extended Data Table 3 | NMR and refinement statistics for protein structures

	Foldit3 (6MSP)
NMR distance and dihedral constraints	
Distance constraints	
Total NOE	2012
Intra-residue	553
Inter-residue	
Sequential ($\|i – j\| = 1$)	505
Medium-range ($\|i – j\| < 4$)	301
Long-range ($\|i – j\| > 5$)	653
Hydrogen bonds	66
Total dihedral angle restraints	
ϕ	59
ψ	59
Structure statistics	
Violations	
Distance constraints (Å)	0.01
Dihedral angle constraints (º)	0.88
Max. dihedral angle violation (º)	7.80
Max. distance constraint violation (Å)	0.66
Structure quality factors (raw score / Z-scores)	
Procheck G-factor (phi/psi only)	-0.09 / -0.04
Procheck G-factor (all dihedrals angles)	-0.14 / -0.83
Verify3D	0.45 / -0.16
Prosall (-ve)	0.91 / 1.08
MolProbity clashscore	17.51 / -1.48
Average pairwise r.m.s. deviation* (Å)	
Heavy	1.52
Backbone	0.71

*Pairwise r.m.s.d. was calculated among 20 refined structures for 'well-defined' residues 21–45, 48–54, 58–76, 81–87 and 90–96.

nature research

Corresponding author(s): David Baker

Reporting Summary

Nature Research wishes to improve the reproducibility of the work that we publish. This form provides structure for consistency and transparency in reporting. For further information on Nature Research policies, see Authors & Referees and the Editorial Policy Checklist.

Statistical parameters

When statistical analyses are reported, confirm that the following items are present in the relevant location (e.g. figure legend, table legend, main text, or Methods section).

n/a	Confirmed	
□	☒	The exact sample size (*n*) for each experimental group/condition, given as a discrete number and unit of measurement
☒	□	An indication of whether measurements were taken from distinct samples or whether the same sample was measured repeatedly
□	☒	The statistical test(s) used AND whether they are one- or two-sided *Only common tests should be described solely by name; describe more complex techniques in the Methods section.*
☒	□	A description of all covariates tested
☒	□	A description of any assumptions or corrections, such as tests of normality and adjustment for multiple comparisons
☒	□	A full description of the statistics including central tendency (e.g. means) or other basic estimates (e.g. regression coefficient) AND variation (e.g. standard deviation) or associated estimates of uncertainty (e.g. confidence intervals)
□	☒	For null hypothesis testing, the test statistic (e.g. *F*, *t*, *r*) with confidence intervals, effect sizes, degrees of freedom and *P* value noted *Give P values as exact values whenever suitable.*
☒	□	For Bayesian analysis, information on the choice of priors and Markov chain Monte Carlo settings
☒	□	For hierarchical and complex designs, identification of the appropriate level for tests and full reporting of outcomes
☒	□	Estimates of effect sizes (e.g. Cohen's *d*, Pearson's *r*), indicating how they were calculated
☒	□	Clearly defined error bars *State explicitly what error bars represent (e.g. SD, SE, CI)*

Our web collection on statistics for biologists may be useful.

Software and code

Policy information about availability of computer code

Data collection	The pre-compiled Foldit game is freely available for download at https://fold.it for Windows, Linux, and Mac. A standalone version of Foldit is also freely available for academic use; for details visit https://fold.it/standalone. Foldit configuration files for all design puzzles are included in the Supplementary Information. The Rosetta software suite was used to perform ab initio prediction calculations; Rosetta is freely available for academic users on Github, and can be licensed for commercial use by the University of Washington CoMotion Express License Program.
Data analysis	Custom Python scripts written to analyze circular dichroism data are included in the Supplementary Information. Protein structures were analyzed with MolProbity (version 4.2). Crystallographic data were analyzed with PHENIX (release 1.101.1-2155) and Coot (v0.8.7 EL). NMR data were analyzed with SPARKY, XEASY, TALOS_N, ASDP, CYANA, PDBStat and PSVS (version 1.5).

For manuscripts utilizing custom algorithms or software that are central to the research but not yet described in published literature, software must be made available to editors/reviewers upon request. We strongly encourage code deposition in a community repository (e.g. GitHub). See the Nature Research guidelines for submitting code & software for further information.

Data

Policy information about availability of data

All manuscripts must include a data availability statement. This statement should provide the following information, where applicable:

- Accession codes, unique identifiers, or web links for publicly available datasets
- A list of figures that have associated raw data
- A description of any restrictions on data availability

The atomic coordinates of Foldit1, Peak6, and Ferredog-Diesel crystal structures, and the Foldit3 NMR structure, have been deposited in the RCSB Protein Data Bank with accession numbers 6MRR, 6MRS, 6NUK and 6MSP, respectively. Chemical shift and NOESY peak list data for Foldit3 were deposited in the Biological Magnetic Resonance Bank (BMRB ID 30527).

Field-specific reporting

Please select the best fit for your research. If you are not sure, read the appropriate sections before making your selection.

☒ Life sciences ☐ Behavioural & social sciences ☐ Ecological, evolutionary & environmental sciences

For a reference copy of the document with all sections, see nature.com/authors/policies/ReportingSummary-flat.pdf

Life sciences study design

All studies must disclose on these points even when the disclosure is negative.

Sample size	Sample size for protein characterization was determined by estimated work load. In total, 146 protein designs were tested, from 97 Foldit puzzles. This was deemed sufficient due to the high number of successfully folded designs in our testing. For in silico designed-backbone analysis, the sample sizes of (n = 717 or 250) was considered sufficient. The inclusion of additional samples is not expected to affect the distribution of measured values.
Data exclusions	No data were excluded from analysis.
Replication	Puzzle configurations were used repeatedly in replicated Foldit puzzles to ensure reproducibility. The final puzzle configuration was used for 25 replicate Foldit puzzles. Protein expression and solubility was tested in duplicate. Structural characterization were performed once or twice with internal statistical validation. If positive results (e.g. protein expression, solubility, etc.) could not be replicated, they are reported as negative results.
Randomization	There was no randomized sample allocation in this work. All tested protein designs received identical treatment.
Blinding	Blinding was not relevant to this work, since all tested proteins received identical treatment.

Reporting for specific materials, systems and methods

Materials & experimental systems

n/a	Involved in the study
☒	☐ Unique biological materials
☒	☐ Antibodies
☒	☐ Eukaryotic cell lines
☒	☐ Palaeontology
☒	☐ Animals and other organisms
☐	☒ Human research participants

Methods

n/a	Involved in the study
☒	☐ ChIP-seq
☒	☐ Flow cytometry
☒	☐ MRI-based neuroimaging

Human research participants

Policy information about studies involving human research participants

Population characteristics	Participation was open and free to the public, and we did not control for participant demographics. See Extended Data Fig. 6 for demographic data from a voluntary (non-obligatory) participant survey.
Recruitment	Participation was open and free to the public, at https://fold.it.